metals

MDPI

Article

Evolution in Microstructure and Mechanical Properties of Inconel 783 Alloy Bolts after Long Term High-Temperature Aging at 700 °C

Peng Duan [1], Zongde Liu [1,*], Shuchao Gu [2] and Song Wang [2]

[1] Key Laboratory of Condition Monitoring and Control for Power Plant Equipment of Ministry of Education, North China Electric Power University, Beijing 102206, China; peng_duan@126.com
[2] Shanghai Minghua Electric Power Science & Technology Co., Ltd., Shanghai 200090, China; gusc@mhdlshanghaipower.com (S.G.); wangs@mhdlshanghaipower.com (S.W.)
* Correspondence: lzd@ncepu.edu.cn; Tel.: +86-010-61772812

Received: 24 September 2020; Accepted: 26 October 2020; Published: 29 October 2020

Abstract: This paper described systematically the changes in microstructure and mechanical properties of Inconel 783 alloy after a considerably long time (equivalently 55,000 h, about 76.4 months) of thermal exposure. Based on the Inconel 783 alloy bolts of an intermediate pressure main stop valve used in a 1000 MW ultra-supercritical unit, the evolution of microstructures and mechanical properties were studied after 700 °C aging temperature with different aging times (1000 h, 3000 h and 20,000 h, corresponding to about 1.4 months, 4.2 months and 27.8 months, respectively), using an optical microscope (OM), scanning electron microscope (SEM), transmission electron microscope (TEM) and X-ray diffractometer (XRD), a universal tensile testing machine and impact testing machine. The results indicated that the bolts aged for 1000 h in two temperatures, showing the second needle β phase, of which the quantity and size obviously increased with aging time. Meanwhile, the characteristics in quantity and shape of the primary β phase changed obviously with the aging time, which transformed to strip the Ni_5Al_3 and Laves-Nb-rich brittle phase in the matrix after aging for 20,000 h. The size of the γ′ phase grew bigger with aging time, and orientation distributions have been observed obviously at 3000 h aging in 700 °C. Compared with the 650 °C aging temperature, the coarsening of γ′ precipitates and second needle β, the orientation distributions of γ′ were more obvious at the 700 °C aging temperature with aging time, which resulted in the rapid decline in yield strength and tensile strength and obvious increase in the brittleness for Inconel 783 alloy bolts.

Keywords: Inconel783 alloy; ultra-supercritical unit; high-temperature aging; microstructure; mechanical properties

1. Introduction

With inlet temperatures of ultra-supercritical steam turbines being up to 600/620 °C, high temperature component design has become a major issue. Among multitudinous high temperature heat-resistant alloys, the Inconel 783 alloy with a low coefficient of thermal expansion (low CTE) and better resistance to stress accelerated grain boundary oxidation (SAGBO) is widely used in fields that require gap control [1–3]. The Siemens company first used Inconel783 alloy as the bolts of turbines in ultra-supercritical (USC) technology [4]. There are three kinds of phase structures in the Inconel 783 alloy including the matrix phase γ, precipitated Al-rich phase β and γ′ phase [5,6], which are the main reasons for the excellent properties of the alloy [7,8]. During last decade, the studies have shown that the microstructure, phase structure and mechanical properties can be changed in long term thermal exposure. Ma et al. [9] and Kang et al. [10] studied the effect of β(NiAl) on fatigue crack propagation

(FCP) of IN783 alloy in a 650 °C environment, pointing out that the SAGBO embrittlement is the principal mechanism of the environmental degradation of the alloy, and highlighted its excellent effect on oxidation resistance and SAGBO resistance. According to the studies of Han et al. [11], investigation was made into the thermo-stability and microstructure of Inconel 783 after long term exposure, respectively, at 650 °C, 700 °C and 750 °C for 1500 h (about 2.1 months), 3000 h (about 4.2 months) and 5000 h (about 6.9 months), and pointed out that the decrease in tensile strength was attributed to the coarsening of the γ′ phase and deterioration of the β phase (the needle Nb-rich phase precipitating within the β phase). Chang et al. [12] placed a high emphasis on the effects of different metallurgical processing on microstructures and mechanical properties of the Inconel 783 alloy, and the experimental results showed that isothermal exposure and heat treatment without aging slightly enhanced the yield strength of alloy 783 at room temperature as well as all metallurgical processing producing an identical stress relaxation behavior at 650 °C.

On the other hand, the failure of Inconel 783 bolts has occurred many times in recent years, which has showed characteristics of suddenness and universality [13–15]. It is necessary to analyze the failure causes comprehensively to guarantee the safe operation of the generator unit. Zhong-Shuai Han [1] studied the evolution of In783 alloy in microstructures and properties enduring up to 48,000 h (about 66.7 months) service time, Han et al. [11] designed the experimental parameters for Inconel 783 alloy up to 5000 h (about 6.9 months) at 750 °C, and Tao et al. [16] selected Inconel 783 bolt samples with service times of 0, 7 and 60 months (about 43,200 h) in a power plant 660 MW Ultra supercritical unit to study the microstructural evolution and mechanical properties. However, there still a lack of an investigation of the evolution of mechanical properties and microstructures of Inconel 783 bolts after a considerably long time of thermal exposure. The investigation of failure modes and failure mechanisms of Inconel 783 alloy bolts is imperative.

In this paper, we focused on the characteristics of microstructural and mechanical properties of Inconel 783 bolts after a considerably long time of thermal exposure (over aging). The bolts of a intermediate pressure main stop which had served 35,000 h (about 48.6 months) in an 1000 MW ultra-supercritical unit were used, and the characteristics of microstructure and mechanical properties were investigated systematically with aging time in 700 °C, compared with the 650 °C aging temperature. The control group samples (defined as "as-initial bolts") that have never been in service were added for a comparison. This research work is devoted to providing valuable information for the actual service, and to investigate the evolution of performance of Inconel 783 alloy bolts with long term high temperature aging.

2. Experiment

2.1. Materials and Heat Treatment

Bolts made of conventional nickel based superalloy Inconel 783 were investigated, which had been subjected a standard heat treatment during their preparation processes in accord with the regular production line by Special Metals Corporation [17]. The following steps were conducted: solution treatment at 1110 °C for 1 h and air cooling, plus a "β age" step at 845 °C for 3 h and air cooling to room temperature, plus age hardening at 720 °C for 8 h and furnace cooling at 55 °C/h to 620 °C for 8 h and air cooling. The experiment bolts were used in the intermediate pressure main stop valve of a 1000 MW ultra-supercritical unit, and were operated at temperature of 603 °C, pressure of 6.0 MPa, respectively. The bolts have served for about 35,000 h during unit operation, and then were further subjected to long term aging for 1000 h, 3000 h and 20,000 h at 700 °C using the muffle furnace. The cylindrical bolt dimensions are M90 mm × 6 mm × 385 mm, and the chemical composition of these materials is listed in Table 1.

Table 1. Chemical compositions of Inconel 783 alloy bolts (mass fraction %).

Element	Ni	Fe	Co	Al	Nb	Ti	Cr
Bolts	28.8 ± 0.4	26.2 ± 0.4	Remainder	5.36 ± 0.3	3.02 ± 0.3	0.20 ± 0.05	3.01 ± 0.3
Special Metals [17]	26.0–30.0	24.0–27.0	Remainder	5.0–6.0	2.5–3.5	0.1–0.4	2.5–3.5

2.2. Characterization

The chemical compositions of the bolts were measured by a spark source atomic emission spectrometer (SPECTROMAXx, SPECTRO GmbH, Kleve, Germany), the evolution of the microstructure was characterized by an optical microscope (OM, Axio Oberver.D1m, Carl Zeiss GmbH, Jena, Germany), scanning electron microscope (SEM, Axio Oberver.D1m, FEI Company, Hillsboro, OR, USA), energy dispersive spectroscopy (EDS, EDAX Inc., Mahwah, NJ, USA) and transmission electron microscope (TEM, TECNAI F30, FEI Company, Hillsboro, OR, USA). In order to investigate the microstructure and identify the phase constitution, X-ray diffraction (XRD, D8 Advance, Bruker Corporation, Karlsruhe, Germany) was applied, using Cu Kα radiation in the 2θ range from 30° to 110°. As regards to mechanical properties, microcomputer control electron universal testing machines (C45.305, MTS Systems Corporation, Eden Prairie, MN, USA) and an impact tester (SANS ZBC2302-B, SANS, Shenzhen, China) were used to test the tensile property and impact toughness, respectively.

All the samples for the tensile test and charpy pendulum impact test have been machined from these bolts after the aging process. To reduce the experimental error and ensure accuracy, three test samples (tensile test and impact test) were prepared in parallel to obtain the average properties, and all samples were taken from the cross sections of same location of the bolts. The tensile test and impact test were carried out at room temperature (25 °C) according to GB/T228.1-2010 and GB/T229-2007 standard, respectively. The gauge length (L_0) of tensile specimen is 50 mm, and the tensile velocity is 2 mm/min. The experimental procedure and collection methods of tensile and impact specimens are shown in Figure 1, and the detailed dimensions are shown in Figure 2.

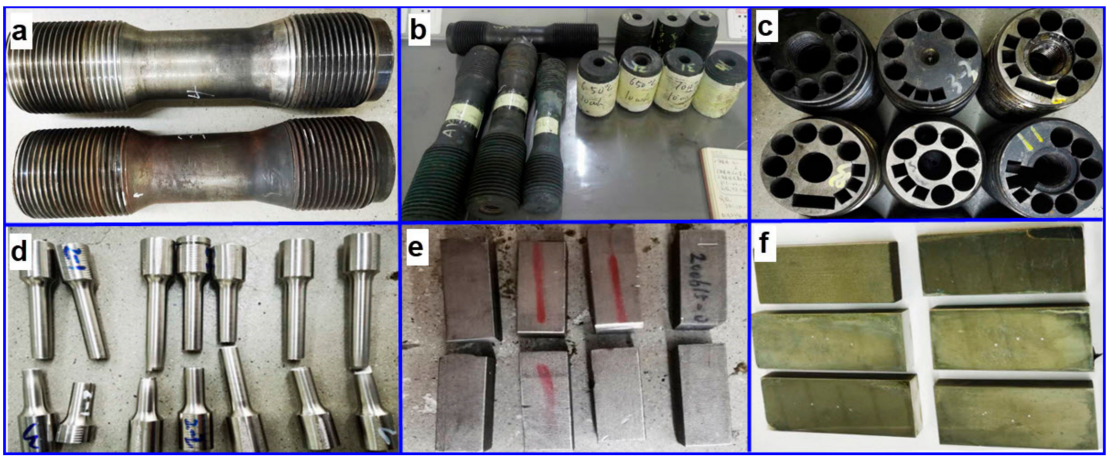

Figure 1. Experimental procedure and sample collection method: (**a**) original bolts sample, (**b**) bolts after aging process, (**c**) bolts after sampling process, (**d**) samples after tensile test, (**e**) samples after impact test, (**f**) samples for microstructural test.

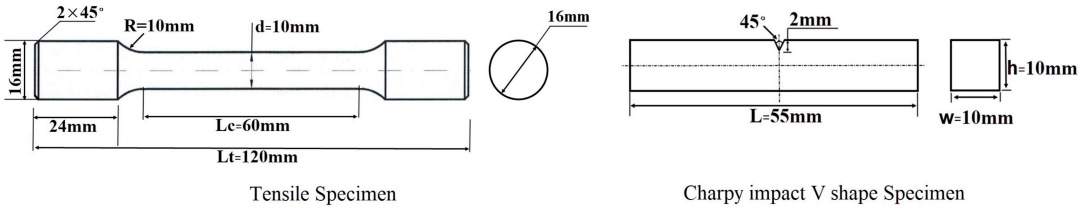

Figure 2. Dimensions of the tensile specimen and impact specimen.

3. Results and Discussion

3.1. Morphology and Microstructure

Figure 3 shows the evolution of Inconel 783 alloy bolts as a function of aging time at 650 °C and 700 °C, respectively. It can be seen that different metallographic structures were present during the aging process. For the as-initial bolt, the β-NiAl phase with block shape was clearly observed, distributing along grain boundaries and within grains as shown in Figure 3a. The secondary needle β phase was observed within the grain boundary for samples after aging 1000 h at 700 °C (Figure 3e), as well as at 650 °C (Figure 3b). The amount of needle β phase had obviously increased after aging 3000 h (Figure 3c,f). With the aging time increased to 20,000 h, the quantity and size of the secondary β phase continuously increased, and the γ grain boundary coarsened significantly simultaneously, as shown in Figure 3d,g. On the other hand, it is evident that the coarsening of the needle β phase was accelerated at the 700 °C with increasing aging time, compared to the 650 °C aging temperature with the same aging time.

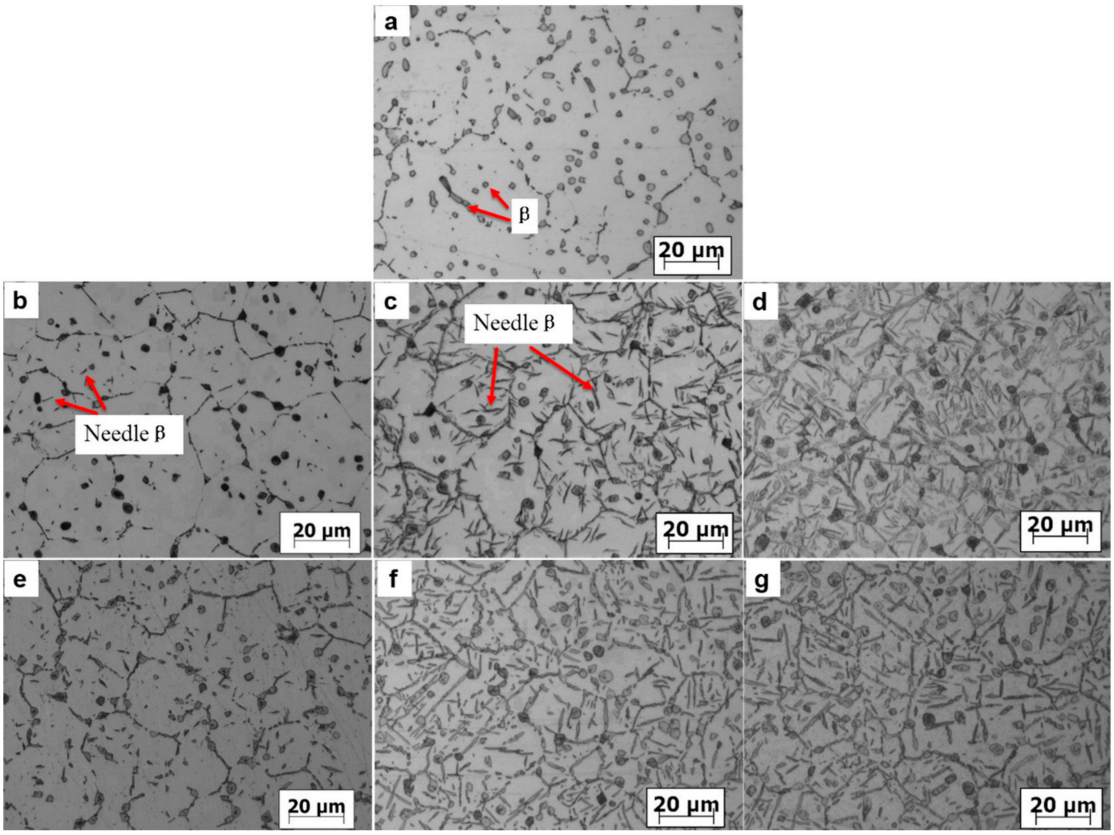

Figure 3. Optical microscope (OM) micrographs of Inconel 783 alloy bolts with different aging temperatures and times: (**a**) 0 h, (**b**) 650 °C—1000 h, (**c**) 650 °C—3000 h, (**d**) 650 °C—20,000 h, (**e**) 700 °C—1000 h, (**f**) 700 °C—3000 h and (**g**) 700 °C—20,000 h.

Figure 4 shows the evolution of SEM microstructures of Inconel 783 alloy after aging 1000 h and 20,000 h at 650 °C and 700 °C, respectively. It is noticeable that the amount and the size of the second needle β phase increased with aging time and temperature, as shown in the red circle marked in Figure 4, which would have a negative effect on the matrix material plasticity due to its anisotropy and concentration of stress. On the other hand, the prior austenite grain boundary was roughened seriously with increased aging time and temperature (marked with the red arrow). Additionally, the coarsening of γ′ precipitates was accelerated with increasing aging temperature, and took place in the way that smaller γ′ precipitates dissolved to promote growth of larger ones, so that resulted in the decrease

in amount and increase in size of γ′ precipitates after aging at 700 °C for 20,000 h (Figure 4h). The γ′ phase could grow with the aging time at 650 °C, however the tendency for growing is not obvious in SEM microstructures. Moreover, the characteristics of the prior β phase have obviously changed with the aging process, showing a decrease in amount and evolution in morphological properties. After aging for 20,000 h at 700 °C, the morphology of the prior β phase changed into a flake shape with a big aspect ratio, as shown in Figure 4h. It has been reported that the chemical composition of the β phase (NiAl-type) in alloy 783 determined by SEM/EDS analysis contained approximately 31% Al by atomic percentage [18], about 17.2% by mass percentage, which was consistent with the Al content (about 17%: mass fraction) of the β phase in the micro zone numbered 2 in this SEM/EDS analysis, as shown in Figure 4k. With the evolution in morphological properties of the prior β phase in aging process, the Al content decreased as shown in Figure 4k, which indicated the degradation of the prior β phase. EDS analysis (Figure 4k) showed that the flake-shape phase with aging 1000 h, 20,000 h at 700 °C contained a high proportion of the Nb (mass fraction: about 10–13%), that was far higher than that of the Inconel 783 alloy matrix (mass fraction: about 3.0%), and this flake-shape phase was also found in samples with aging of 20,000 h at 650 °C. G.W. Han also found this Nb-rich Laves phase in Inconel 783 alloy after long term exposure at 750 °C for 1000 h [5].

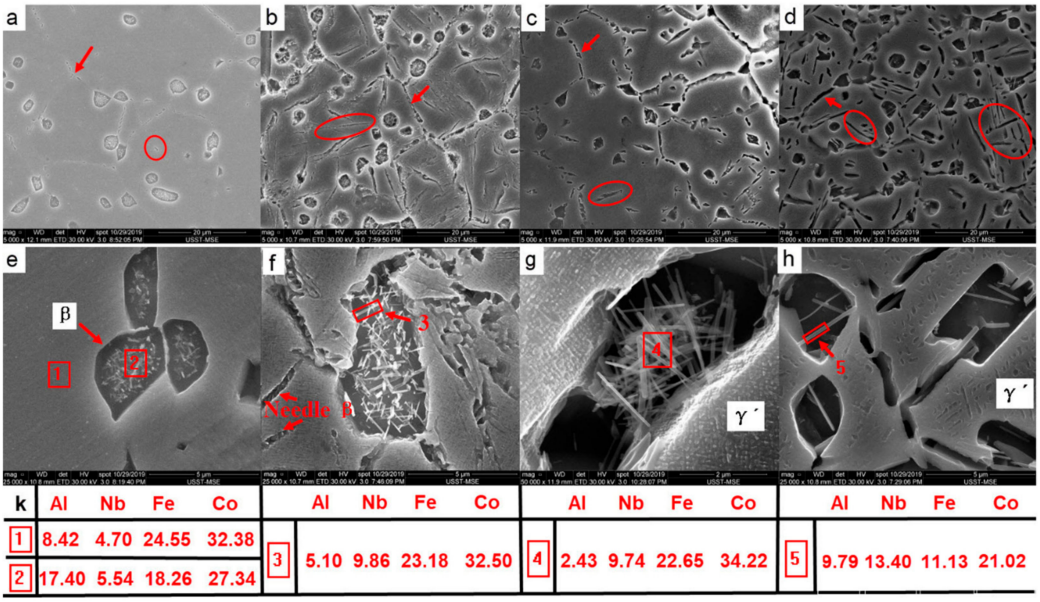

Figure 4. SEM micrographs of the β phase for Inconel 783 alloy bolts with different aging temperatures and times: (**a**,**e**) 650 °C—1000 h, (**b**,**f**) 650 °C—20,000 h, (**c**,**g**) 700 °C—1000 h, (**d**,**h**) 700 °C—20,000 h, and (**k**) EDS analysis of the β phase in micro zones 1,2,3,4,5, respectively.

To further understand the evolution of the γ′ phase and degradation of the β phase that are difficult to observe in OM or SEM microphotographs, TEM was used to analyze the microstructure evolution of Inconel 783 alloy bolts with different aging processes. Figure 5 shows the TEM images of the γ′ phase of Inconel 783 bolts with different time and temperatures. As observed in Figure 5, the dispersive γ′ precipitates increased slightly after aging at 650 °C for 1000 h, showing cubodal particles with an average size of about 50 nm (as shown in Figure 5b), but increased obviously at 700 °C for 1000 h and 20,000 h. Additionally, the growth of γ′ precipitates showed an obvious grain preferred orientation for samples aged at 700 °C, as shown in Figure 5d,e. After aging at 700 °C for 20,000 h, the γ′ precipitates grew extraordinarily and partly interlinked together, showing a marked deterioration characteristic (Figure 5e).

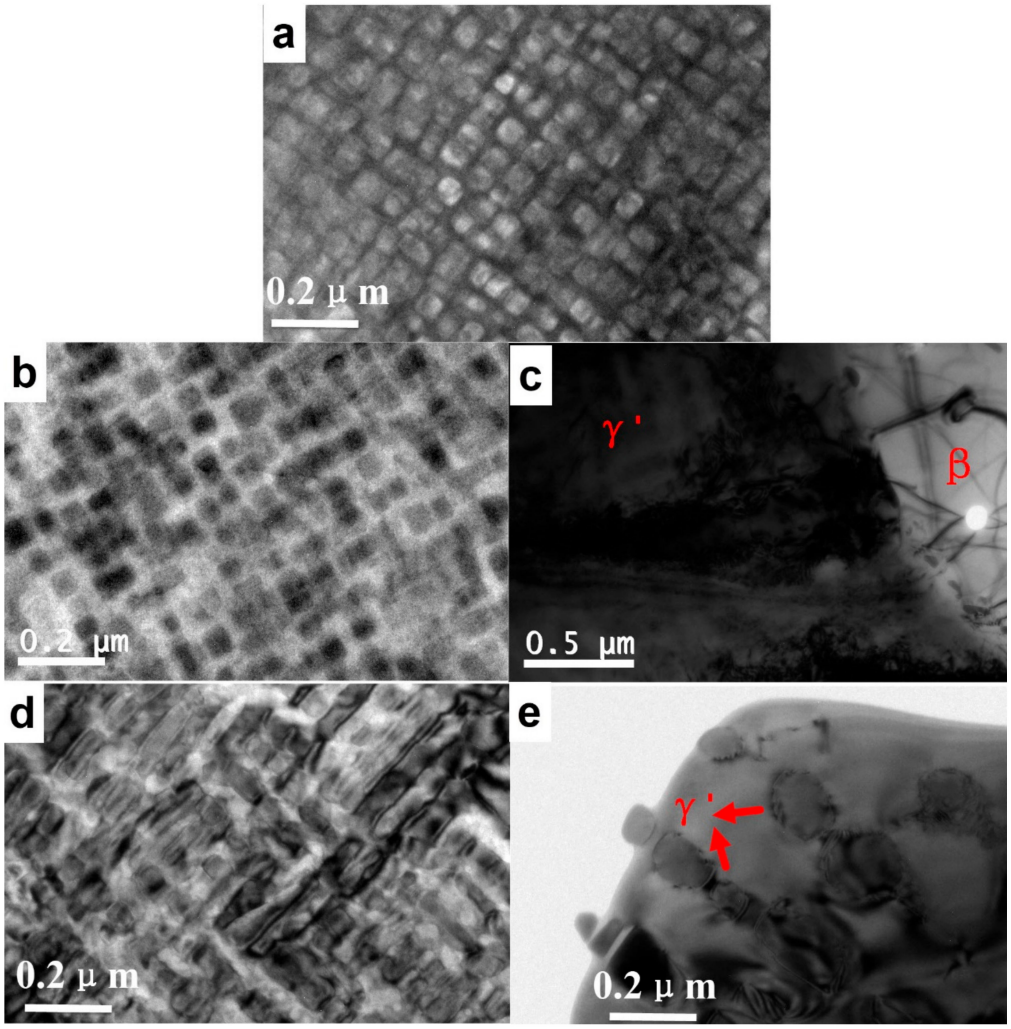

Figure 5. TEM micrographs of the γ′ phase for Inconel 783 alloy bolts with different aging temperatures and times: (**a**) as-initial bolt, (**b**) 650 °C—1000 h, (**c**) 650°C—20,000 h, (**d**) 700 °C—1000 h and (**e**) 700 °C—20,000 h, respectively.

Figure 6 shows the TEM images of the β phase of Inconel 783 bolts for 20,000 h aging at 650 °C. Similarly, the β phase structure, bright field image of the precipitated phase and their dark field images are listed in Figure 6a,b, respectively. Besides the existence of the rich Nb Laves phase observed in SEM and EDS results, another precipitated phase Ni_5Al_3 was observed, which had been verified during service [19,20]. Previous published work [21] indicated that the Ni_5Al_3 could be formed during aging at about 500 °C for days and weeks. Figure 6a also exhibited the interaction of precipitate phases in β and the dislocation, and a clear structure of dislocation tangle was observed in the β phase after 20,000 h at 650 °C. In addition, the γ′ around the β phase was eliminated drastically after aging 20,000 h at 650 °C and 700 °C, respectively, as showed in SEM images (Figure 4h) and later Figure 7.

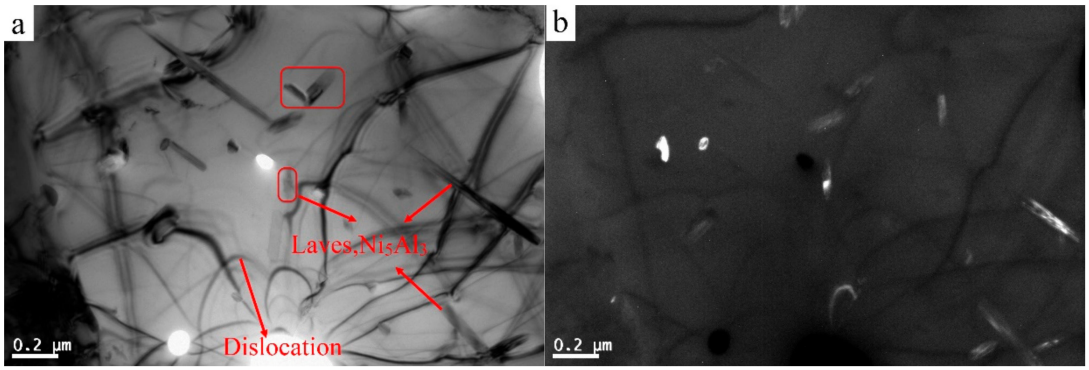

Figure 6. The bright field image (**a**) and dark field image (**b**) of TEM micrographs of the β phase with aging for 20,000 h at 650 °C.

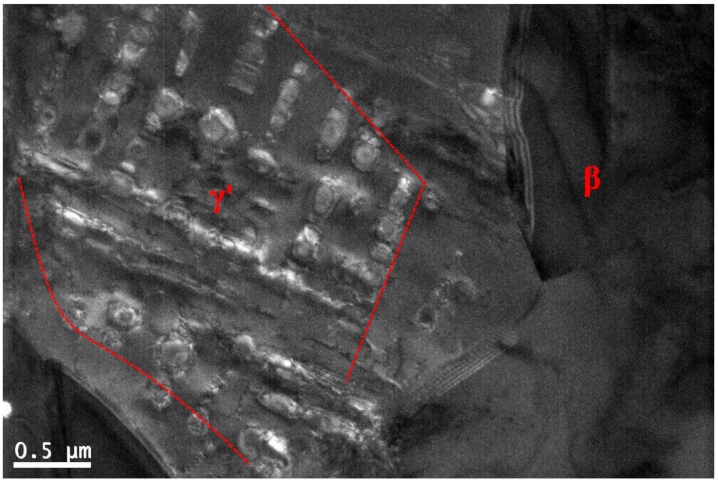

Figure 7. TEM micrographs of the γ′ phase for Inconel 783 alloy bolts after 20,000 h aging at 700 °C. The red line shows the depleted area of γ′ phase around the β phase.

The examination of diffraction peaks by means of XRD proved the formation of an Ni_5A1_3 phase after aging for 1000 h at 650 °C [22], as shown in Figure 8. The XRD result in 650 °C is quoted from our previous research [23]. It could be seen that the as-initial Inconel 783 bolt consisted of β-NiA1 with a bcc structure associated with about 44.0° and γ′ with an fcc structure associated with about 74.7° and 90.7°, respectively. After aging for 1000 h, the appearance of diffraction peaks of Ni_5A1_3 phase associated with about 50.8° was evident in comparison with the XRD pattern of the as-initial samples, indicating the occurrence of the formation of an Ni_5A1_3 phase during the aging process. The other obvious change in XRD patterns was the enhancement of diffraction peaks, associated with about 50.8° and 82.3°, which was attributed to the second β phase taking place in the aging process. Moreover, the diffraction peaks associated with 74.7° and 90.7° had a tendency of narrowing with the aging time increased as shown in Figure 8a,b, which suggested the increment of size of γ′ during the aging process [24,25]. The relationship between average grain size and width of the peaks can be described by the Scherrer theory [26] and Hall–Williamson equations [27], and the average grain size increases with decreasing full width at half-maximum (FWHM) of the peaks. Moreover, the diffraction peaks corresponding to γ′ present a shift to higher angles for samples aged for 20,000 h at 700 °C, compared to the samples aged for 1000 h at 650 °C. That may be caused by the directional distribution of phase γ′ in the process of high-temperature aging, as observed in SEM and TEM microstructures after 1000 and 20,000 h aging at 700 °C.

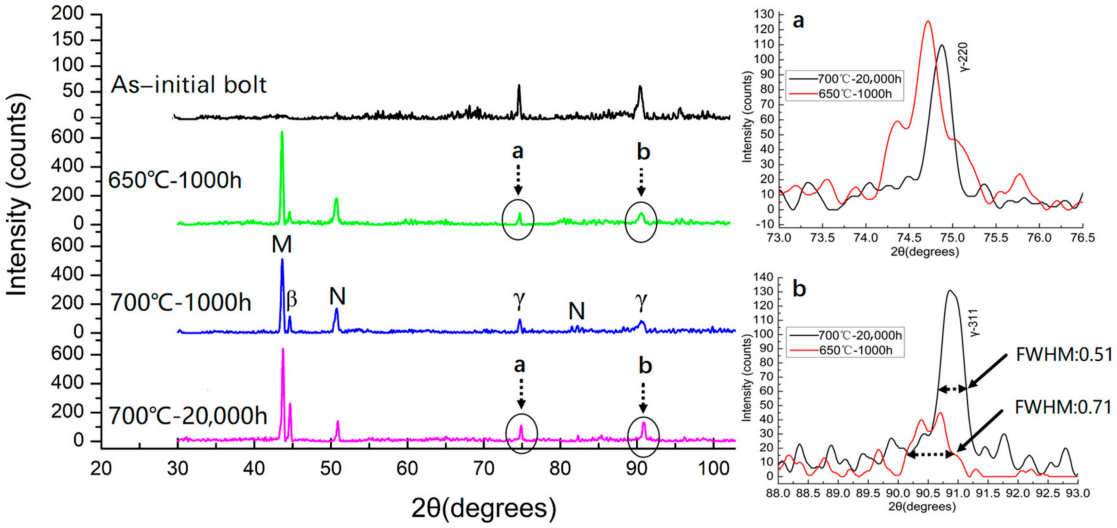

Figure 8. The evolution of the XRD line profile of Inconel 783 alloy bolts with different aging processes (γ-Austenite, N-Ni_5Al_3, β-Second needle β, M-martensite), and the magnifying diffraction peaks of γ′ phase associated with 74.7° and 90.7° for the samples after 1000 h aging at 650 °C (**a**) and 20,000 h aging at 700 °C (**b**).

It is well known that the Inconel 783 alloy primarily consists of three phases, γ′-Ni_3Al, β-NiA1, and the γ austenitic phase as the matrix. The transformation of the β-NiA1 phase and γ′ phase into the Ni_5Al_3 phase is shown in the reaction: 2β-NiA1 + γ′-Ni_3Al → Ni_5Al_3 [19]. The Al-enriched β phase, distributing along grain boundaries and within grains, can react with oxygen and form Al_2O_3 to prevent further oxidation at elevated temperature (597–897 °C), and play an important role in enhancing the resistance to SAGBO-induced cracking [9]. The fine particles of γ′ phase in alloy 783 precipitated homogeneously can ensure the high strength of the alloy matrix [7]. Therefore, the formation of the Ni_5Al_3 phase not only deteriorates the strength of the β phase, but also results in severe oxygen embrittlement for the material [28,29].

3.2. Mechanical Properties

Figure 9 shows the results of tensile property assessment at room temperature for specimens subjected to different aging treatments [23]. After the aging treatment at 650 °C and 700 °C, Inconel 783 alloy bolts showed a decrease in yield strength and tensile strength with different aging times, compared to the as-initial bolts. Specifically, the specimens showed the highest yield strength (855.3 MPa) and tensile strength (1242.3 MPa) for 3000 h aging at 650 °C and presented the lowest tensile strength (1158.0 MPa) for 20,000 h aging. The tensile property of samples aged at 700 °C exhibited a significant deterioration in different aging processes (compared to the reference value of 779 MPa and 1197 MPa at 21 °C, given by the Special Metals of Special Metals Corporation), showing a clear decrease in yield strength and tensile strength. The yield strength and tensile strength for samples aged for 20,000 h decreased to 585.0 MPa and 974.0 MPa, from 773.3 MPa and 1158.0 MPa for samples aged for 1000 h (almost 24.35% and 15.89% decreases, respectively).

Impact toughness measurements, as a function of aging time at 650 °C and 700 °C, are plotted in Figure 10 [23]. It can be seen that the as-initial Inconel 783 alloy bolts exhibit a value of 24.7 KV_2/J, that is similar to results (25.33 KV_2/J) reported by Peng Yichao [13]. With the extension of aging time, the impact toughness showed a sequential decline for all samples aged at 650 °C and 700 °C, indicating the severe embrittlement of the material.

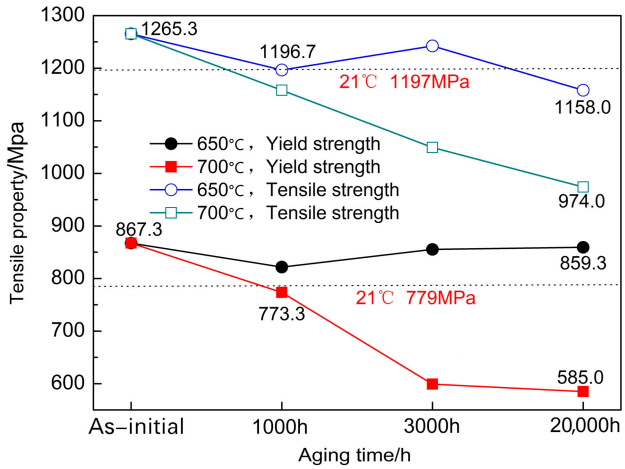

Figure 9. Mechanical properties at room temperature of Inconel 783 alloy bolts for different aging times and temperatures.

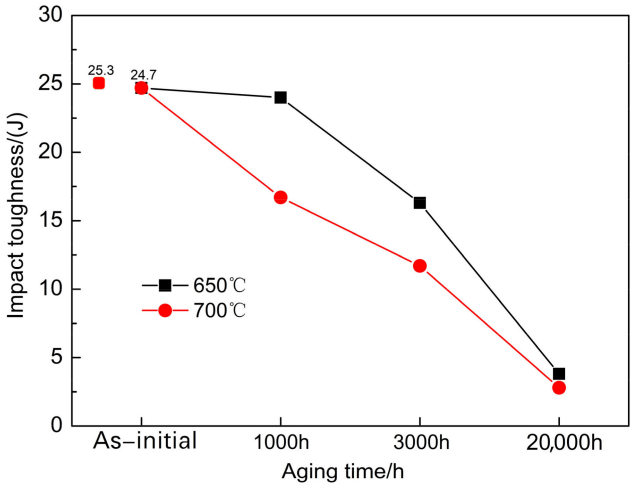

Figure 10. Impact properties at room temperature of Inconel 783 alloy bolts for different aging times and temperatures.

Figure 11 shows the representative tensile fracture morphologies of the Inconel 783 bolts using low magnification SEM. It is clear that two distinct morphologies can be identified on the fracture surface of tensile specimens: (i) the brittle fracture features, showing a distinct herringbone in the extension area initiated in surface layer as marked with a red arrow, and (ii) the shear zone attributed to the plastic deformation around the edge zone. With the extension of aging time, the proportion of the brittle zone increased markedly, approximately 100% in the fracture surface after aging for 20,000 h at 650 °C and 700 °C, indicating the increase in the brittleness for Inconel 783 bolts with the aging time and temperature. That is consistent with the evolution of the impact toughness property indicated by Figure 10. Furthermore, it could be found from the fractography shown in Figure 12 that the characteristics of the grain boundary of the samples aged for 20,000 h at 650 °C and 700 °C changed to the shape with an irregular strip from the almost round shape for the bolts with aging for 1000 h at 650 °C and 700 °C, indicating that the grain boundary strength of the γ and second needle β gradually broke. The coarse grain boundary of the needle β and initial grain boundaries of the γ matrix may act as a fracture nucleation core, becoming the zone with a low bearing capacity for the crack initiation, extension and fracture during the tensile test.

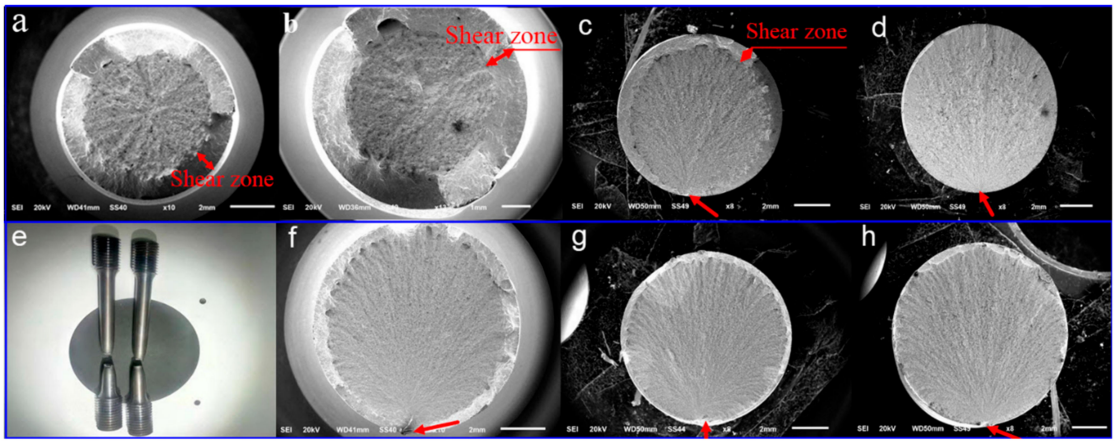

Figure 11. Macrographs for tensile fracture morphology of Inconel 783 alloy bolts that were as-initial (**a**), and aged at 650 °C for 1000 h (**b**), 3000 h (**c**), 20,000 h (**d**), and 700 °C for 1000 h (**f**), 3000 h (**g**), and 20,000 h (**h**), and samples after the tensile test (**e**).

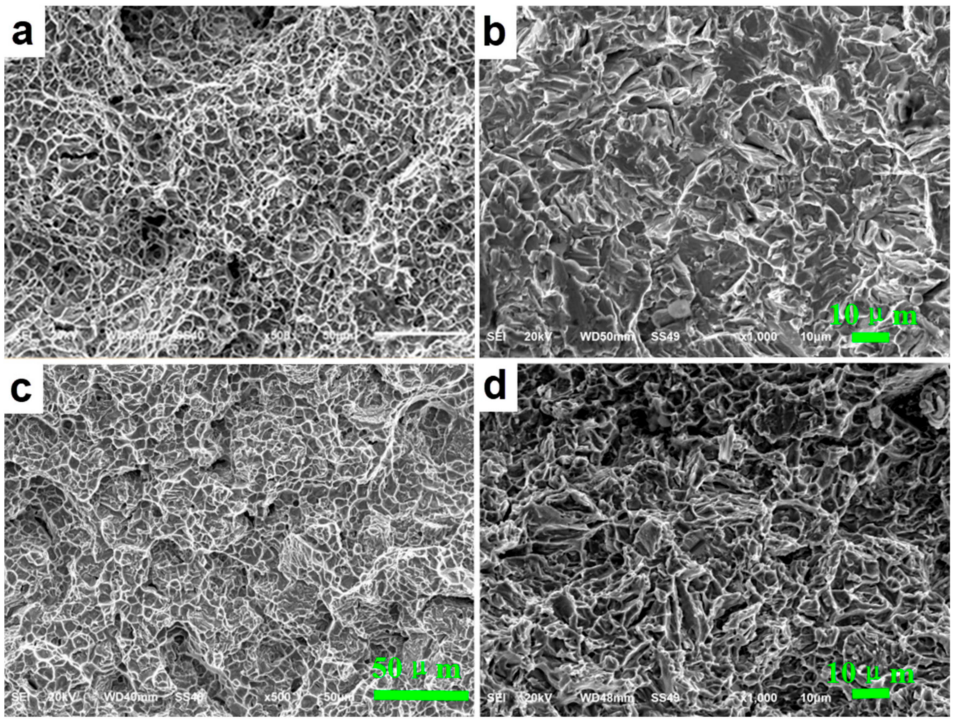

Figure 12. SEM images for tensile fracture morphology of Inconel 783 alloy bolts after aging at 650 °C for 1000 h (**a**), 20,000 h (**b**), and 700 °C for 1000 h (**c**), 20,000 h (**d**).

4. Conclusions

The evolution of microstructure and mechanical properties of the Inconel 783 alloy bolts with different aging times at 650 °C and 700 °C were investigated in this paper. Microstructure analysis highlighted the formation of a needle β phase along the grain boundaries of primary γ, and the scale of changes in grain size, amount, and shape for the needle β phase with the extension of the aging process. With increasing aging temperature and time, the preferred orientation of γ′ became intensified, accompanied by the increase in size of the γ′ phase. Moreover, continued aging led to the increase in precipitation of the Ni_5Al_3 phase and Nb-rich Laves phase, resulting in rapid deterioration of β phase, and brittleness of the materials and low ductility.

As for mechanical properties, the strength of the bolts decreased slightly after aging at 650 °C with different aging times and presented the minimum value of tensile strength (1158.0 MPa) after

20,000 h aging. Aging at 700 °C lead to a significant reduction in strength at room temperature due to the excessive coarsening of γ′ precipitates and the increasing amount of the second needle β phase. In addition, all Inconel 783 alloy bolts showed an obvious increase in the brittleness, that was attributed to the formation of the Ni_5Al_3 phase and the deterioration of the β phase. Moreover, the grain boundary becomes more fragile during high temperature aging.

The metallographic structure of Inconel 783 alloy bolts changed clearly for different aging processes at 650 °C and 700 °C (particularly the formation and variation of the second needle β phase), which could contribute to assessment of the performance and usability of the Inconel 783 alloy bolts at service.

Author Contributions: Conceptualization, Z.L.; Formal analysis, P.D., Z.L., S.G. and S.W.; Funding acquisition, Z.L.; Investigation, P.D., Z.L., S.G. and S.W.; Methodology, S.G.; Project administration, P.D.; Supervision, S.W.; Writing—original draft, P.D. and S.G.; Writing—review and editing, Z.L. All authors have read and agreed to the published version of the manuscript.

Funding: This research was funded by the the Science and Technology Project (project number 33002599170707) surpported by Shanghai Minghua Electric Power Science & Technology Co., Ltd.

Conflicts of Interest: The authors declare no conflict of interest.

References

1. Han, Z.S.; Du, J.F.; Liang, J.; Zhang, Z. Evolution of In783 alloy in microstructure and properties enduring different service times. *Rare Met.* **2018**, 1–8. [CrossRef]
2. Nagesha, A.; Goyal, S.; Valsan, M.; Rao, K.B.S.; Mannan, S.K. Low cycle fatigue behaviour of InconelR alloy 783. *Trans. Indian Inst. Met.* **2010**, *63*, 575–579. [CrossRef]
3. Ma, L.; Chang, K.; Mannan, S.K. Oxide-induced crack closure: An explanation for abnormal time-dependent fatigue crack propagation behavior in Inconel alloy 783. *Scr. Mater.* **2003**, *48*, 583–588. [CrossRef]
4. Heck, K.A.; Smith, J.S.; Smith, R. Inconel Alloy 783: An Oxidation Resistant, Low Expansion Superalloy for Gas Turbine Applications. *J. Eng. Gas Turbines Power* **1998**, *120*, 128–132. [CrossRef]
5. Han, G.W.; Zhang, Y.Y. Variations in microstructure and properties of GH783 alloy after long term thermal exposure. *Mater. Sci. Eng. A* **2006**, *441*, 253–258. [CrossRef]
6. Mannan, S.K.; Smith, G.D.; Patel, S.J. Thermal stability of Inconel alloy 783 at 593 °C and 704 °C. *Superalloys 2004* **2004**, 627–635.
7. Nagesha, A.; Goyal, S.; Nandagopal, M.; Parameswaran, P.; Sandhya, R.; Mathew, M.D.; Mannanc, S.K. Dynamic strain ageing in Inconel Alloy 783 under tension and low cycle fatigue. *Mater. Sci. Eng. A* **2012**, *546*, 34–39. [CrossRef]
8. Sharghi-Moshatghin, R.; Asgari, S. The effect of thermal exposure on the γ′ characteristics in a Ni-base superalloy. *J. Alloys Compd.* **2004**, *368*, 144–151. [CrossRef]
9. Ma, L.; Chang, K.M.; Mannan, S.K. Effects of NiAl-β precipitates on fatigue crack propagation of Inconel alloy 783 under time-dependent condition with various load ratios. *Scr. Mater.* **2003**, *48*, 551–557. [CrossRef]
10. Kang, B.; Liu, X.; Cisloiu, C.; Chang, K.M. High temperature moiré interferometry investigation of creep crack growth of inconel 783-environment and β-phase effects. *Mater. Sci. Eng. A* **2003**, *347*, 205–213. [CrossRef]
11. Han, G.W.; Dun, B.; Yang, Y.J. Investigation on Thermal Stability of Oxidation Resistant Low Thermal Expansion Superalloy Inconel 783 after Long Term Thermo-exposure. *J. Iron Steel Res.* **2011**, *23*, 278–281.
12. Ma, L.; Chang, K. Effects of Different Metallurgical Processing on Microstructures and Mechanical Properties of Inconel Alloy 783. *J. Mater. Eng. Perform.* **2004**, *12*, 32–38. [CrossRef]
13. Peng, Y.C.; Lou, Y.M.; Xu, S.P. Fracture failure analysis on Alloy783 bolts in medium-pressure valve bonnets of USC units. *Therm. Power Gener.* **2018**, *47*, 115–122.
14. Jia, R.F.; Li, L.; Qin, C.P. Failure Analysis of IN783 Alloy Bolt Used on 1000MW Ultra Supercritical Steam Turbine. *Turbine Technol.* **2018**, *61*, 78–81.
15. Luo, C.; Qian, Y.J.; Liu, J.J. Fracture Cause of Inconel783 Alloy Bolt in Medium-Pressure Contronl Valve of Ultra-supercritical Unit. *Mater. Mech. Eng.* **2019**, *43*, 71–79.
16. Jiang, T.; Chen, L.; Jiang, F.; Cai, H.; Sun, J. Microstructural evolution and mechanical properties of a nickel-based superalloy through long-term service. *Mater. Sci. Eng. A* **2016**, *656*, 184–189. [CrossRef]

17. Special Metals. INCONEL®Alloy 783. Publication Number SMC-064. 2004. Available online: www.specialmetals.com (accessed on 18 October 2020).
18. Mannan, S.; Debarbadillo, J. Long Term Thermal Stability of Inconel Alloy 783. In Proceedings of the ASME 1998 International Gas Turbine and Aeroengine Congress and Exhibition, Stockholm, Sweden, 2–5 June 1998.
19. Li, C.F.; Ren, Y.P.; Qin, G.W. Experimental confirmation of Ni5Al3 phase in Ni-Al binary system by diffusion couple technique. *Adv. Mater. Res. 299–300*, 224–227.
20. Robertson, M.; Wayman, C.M. Ni5Al3 and the nickel-aluminum binary phase diagram. *Metallography* **1984**, *17*, 43–55. [CrossRef]
21. Khadkikar, P.S.; Vedula, K. An investigation of the Ni5Al3 phase. *J. Mater. Res.* **1987**, *2*, 163–167. [CrossRef]
22. Cheng, T. Ni5Al3 phase in heat cycled nickel-rich NiAl. *J. Mater. Sci. Lett.* **1996**, *15*, 285–289. [CrossRef]
23. Duan, P.; Liu, Z.; Li, B.; Wang, Q.; Gu, S. Effect of aging at 650 °C on microstructure and mechanical properties of GH783 alloy bolts. *Eng. Fail. Anal.* **2020**, *118*, 104853. [CrossRef]
24. Duan, Y.P.; Gu, S.C.; Zhang, Z.G.; Wen, M. Characterization of structures and novel magnetic response of Fe87.5Si7Al5.5 alloy processed by ball milling. *J. Alloys Compd.* **2012**, *542*, 90–96. [CrossRef]
25. Duan, Y.P.; Zhang, Y.H.; Wang, T.G.; Gu, S.C.; Li, X.; Lv, X.J. Evolution study of microstructure and electromagnetic behaviors of Fe-Co-Ni alloy with mechanical alloying. *Mater. Sci. Eng. B* **2014**, *185*, 86–93.
26. Robertson, J.H. Elem. of x-ray diffraction by BD Cullity. *Acta Crystallogr. Sect. A Cryst. Phys. Diffr. Theor. Gen. Crystallogr.* **1979**, *35*, 350.
27. Burton, A.W.; Ong, K.; Rea, T.; Chan, I.Y. On the estimation of average crystallite size of zeolites from the scherrer equation: A critical evaluation of its application to zeolites with one dimensional pore systems. *Microporous Mesoporous Mater.* **2009**, *117*, 75–90. [CrossRef]
28. Qi, H.Y.; Yang, J.S.; Yang, X.G.; Li, S.L. Low-cycle fatigue behavior of a directionally solidified Ni-based superalloy subjected to gas hot corrosion pre-exposure. *Rare Met.* **2019**, *38*, 227–232. [CrossRef]
29. Yang, J.H.; Wayman, C.M. On the Ni5Al3 phase and yield strengthated phenomena in a NiAlFe alloy. *Mater. Sci. Eng. A* **1993**, *160*, 241–249. [CrossRef]